

PTEN deletion enhances the regenerative ability of adult corticospinal neurons

Kai Liu^{1,4}, Yi Lu^{1,4}, Jae K Lee², Ramsey Samara², Rafer Willenberg³, Ilse Sears-Kraxberger³, Andrea Tedeschi¹, Kevin Kyungsuk Park¹, Duo Jin¹, Bin Cai¹, Bengang Xu¹, Lauren Connolly¹, Oswald Steward³, Binhai Zheng² & Zhigang He¹

Despite the essential role of the corticospinal tract (CST) in controlling voluntary movements, successful regeneration of large numbers of injured CST axons beyond a spinal cord lesion has never been achieved. We found that PTEN/mTOR are critical for controlling the regenerative capacity of mouse corticospinal neurons. After development, the regrowth potential of CST axons was lost and this was accompanied by a downregulation of mTOR activity in corticospinal neurons. Axonal injury further diminished neuronal mTOR activity in these neurons. Forced upregulation of mTOR activity in corticospinal neurons by conditional deletion of *Pten*, a negative regulator of mTOR, enhanced compensatory sprouting of uninjured CST axons and enabled successful regeneration of a cohort of injured CST axons past a spinal cord lesion. Furthermore, these regenerating CST axons possessed the ability to reform synapses in spinal segments distal to the injury. Thus, modulating neuronal intrinsic PTEN/mTOR activity represents a potential therapeutic strategy for promoting axon regeneration and functional repair after adult spinal cord injury.

Spinal cord injury often results in permanent paralysis, largely as a result of the failure of injured axons to regenerate in the adult mammalian CNS. In principle, functional recovery after CNS injury could be achieved by two forms of axonal regrowth: sprouting of spared non-injured axons to form new circuits compensating for the lost functions and regeneration of lesioned axons that can potentially re-form the lost connections^{1,2}. Of the different types of long-projecting descending tracts, the CST that controls voluntary movements is particularly important for functional recovery after spinal cord injury^{3,4}. Despite numerous efforts to stimulate both collateral and regenerative growth of CST axons in experimental injury models^{1–4}, success has been very limited^{5–7}, suggesting that injured CST axons are particularly refractory to regeneration. For example, removing extracellular inhibitory molecules allows some sprouting of spared CST axons but very limited regeneration of injured axons^{8–10}. Delivery of neurotrophic factors promotes some degree of regeneration in certain types of axons, such as optic nerve axons from retinal ganglion neurons¹¹ but fails to elicit regeneration of injured CST axons after spinal cord injury^{12,13}. Overexpressing the BDNF receptor TrkB can promote CST axon regrowth into a BDNF-expressing graft after a subcortical injury¹⁴, but it is unknown whether this finding can be extended to spinal cord injury. Furthermore, although grafting permissive substrates at the spinal cord injury site permits some sensory axons and brain-stem-derived axons to grow into the graft, CST axons show minimal growth^{15,16}. Even at early postnatal stages, most injured CST axons fail to grow into a permissive graft, although axons of other neural systems

are capable¹⁷. These findings have instilled doubt as to whether it is even possible to develop a strategy for stimulating regeneration of large numbers of injured CST axons after spinal cord injury.

We recently discovered that age- and injury-dependent down-regulation of neuronal mTOR activity is a major cause of the lack of regeneration of optic nerve axons after injury and that genetic activation of mTOR promotes successful optic axon regeneration¹⁸. However, it is unknown whether this is specific to retinal ganglion neurons or applicable to other CNS neurons. We found that enhancement of the mTOR pathway enhanced regrowth (both sprouting and regeneration) of adult CST axons in different types of injury models.

RESULTS

Correlation between mTOR levels and CST sprouting

We first investigated whether mTOR activity regulates the sprouting responses of CST axons after unilateral pyramidotomy^{19,20} (**Supplementary Fig. 1**). In this model, the CST was severed unilaterally at the left medullary pyramid above the pyramidal decussation. The anterograde tracer biotinylated dextran amine (BDA) was injected into the right sensorimotor cortex to label uninjured CST axons. In intact mice, most labeled axons were detected on the left side of the spinal cord, with few axons appearing in the right side (**Fig. 1**). Thus, increased numbers of labeled axons in the right side of the spinal cord following a pyramidotomy would represent transmidline sprouting of intact CST axons into the denervated side.

¹F.M. Kirby Neurobiology Center, Children's Hospital, and Department of Neurology, Harvard Medical School, Boston, Massachusetts, USA. ²Department of Neurosciences, University of California San Diego, La Jolla, California, USA. ³Reeve-Irvine Research Center, University of California at Irvine College of Medicine, and Department of Anatomy & Neurobiology, Neurobiology & Behavior and Neurosurgery, Irvine, California, USA. ⁴These authors contributed equally to this work. Correspondence should be addressed to Z.H. (zhigang.he@childrens.harvard.edu).

Received 22 April; accepted 23 June; published online 8 August 2010; doi:10.1038/nn.2603

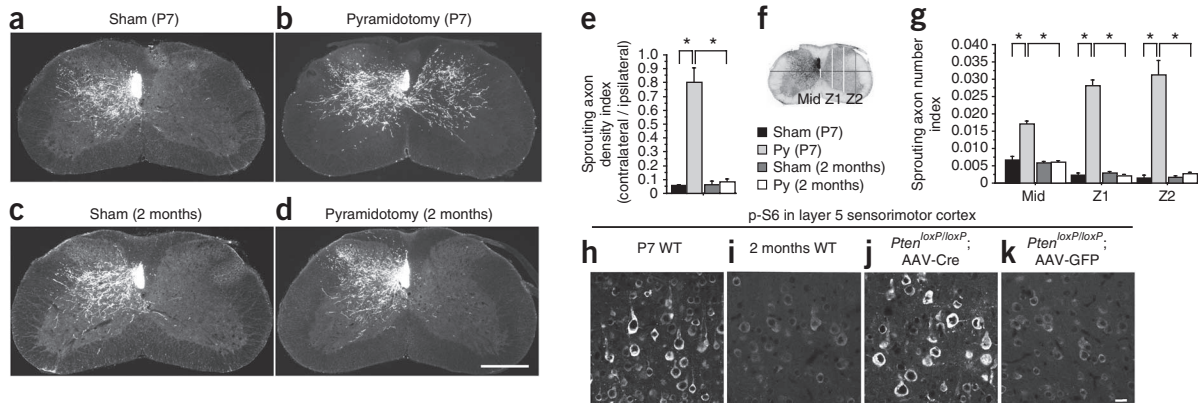


Figure 1 Correlation between age-dependent decrease of CST sprouting and phospho-S6 levels in corticospinal neurons. **(a–d)** Representative images of cervical 7 (C7) spinal cord transverse sections from wild-type mice with a left pyramidotomy (Py) performed at P7 **(b)** or 2 months **(d)** and their respective controls **(a,c)**. BDA was injected into the right sensorimotor cortex at 2 weeks post-injury and mice were killed 2 weeks later. Scale bar represents 500 μ m. **(e)** Quantification of sprouting axon density index (contralateral/ipsilateral). * $P < 0.01$, ANOVA followed by Bonferroni's *post hoc* test. **(f)** Scheme of quantifying crossing axons at different regions of the spinal cord. Mid, midline; Z1 and Z2, different lateral positions. **(g)** Quantification results with the methods indicated in **f** and then normalized to total numbers of labeled CST axons counted at the medulla in each mouse. * $P < 0.01$, ANOVA followed by Bonferroni's *post-hoc* test. For the quantification results in **e–g**, we used four mice in each of the control groups, five mice in the P7 groups and seven mice in the 2 months groups. Three sections at the C7 level were quantified per mouse. **(h–k)** Representative images of the coronal sections of the layer 5 sensorimotor cortex from wild-type mice at P7 **(h)**, 2 months **(i)** or 2-month-old *Pten*^{loxP/loxP} mice of with AAV-Cre **(j)** or AAV-GFP **(k)**. Scale bar represents 20 μ m.

Using this procedure, we found a sharp age-dependent decline in trans-midline sprouting responses, whereas left pyramidotomy at postnatal day 7 (P7) induced massive trans-midline sprouting of CST axons from the uninjured side (**Fig. 1b,e,g**), the same injury in 2-month-old mice led to minimal CST sprouting (**Fig. 1d,e,g**). To assess mTOR activity in cortical neurons of different ages, we performed immunohistochemistry on cortical sections using antibody to phospho-S6 (p-S6), an established marker of mTOR activation¹⁸. Immunostaining for p-S6 was markedly reduced in most of adult cortical neurons (**Fig. 1i**) compared with that in P7 brains (**Fig. 1h**), suggesting that there is a correlation between the downregulation of the mTOR activity and the decrease in the compensatory sprouting ability of cortical neurons.

Pten deletion increases CST sprouting

We next examined whether preventing the age-dependent mTOR downregulation could enhance the sprouting responses of adult CST axons. We used Cre-expressing adeno-associated virus (AAV-Cre) to delete *Pten*, a negative regulator of mTOR²¹, in homozygous conditional *Pten* mutant (*Pten*^{loxP/loxP}) mice²². As a validation of the strategy, we found that injection of AAV-Cre, but not AAV-green fluorescent protein (GFP) virus, into the sensorimotor cortex of a Cre reporter mouse (Rosa26-loxP-STOP-loxP-PLAP²³) induced efficient Cre-dependent placental alkaline phosphatase (PLAP) expression in neurons throughout the sensorimotor cortex (**Supplementary Fig. 2**).

To assess whether *Pten* deletion elevates neuronal mTOR activity, we injected AAV-Cre into the sensorimotor cortex of *Pten*^{loxP/loxP} mice at P1 and examined the p-S6 signal in the adult. Indeed, compared with AAV-GFP-injected *Pten*^{loxP/loxP} controls (**Figs. 1k** and 2), immunostaining for p-S6 was substantially higher in adult *Pten*-deleted cortical neurons (**Figs. 1j** and 2). This postnatal AAV-Cre-mediated *Pten* deletion does not appear to alter the projections of CST axons in the spinal cord, as the numbers and termination patterns of labeled axons in the pyramids and different levels of spinal cord were not substantially different in the *Pten*^{loxP/loxP} mice injected with either AAV-Cre or AAV-GFP (**Supplementary Fig. 3**). This result is consistent with

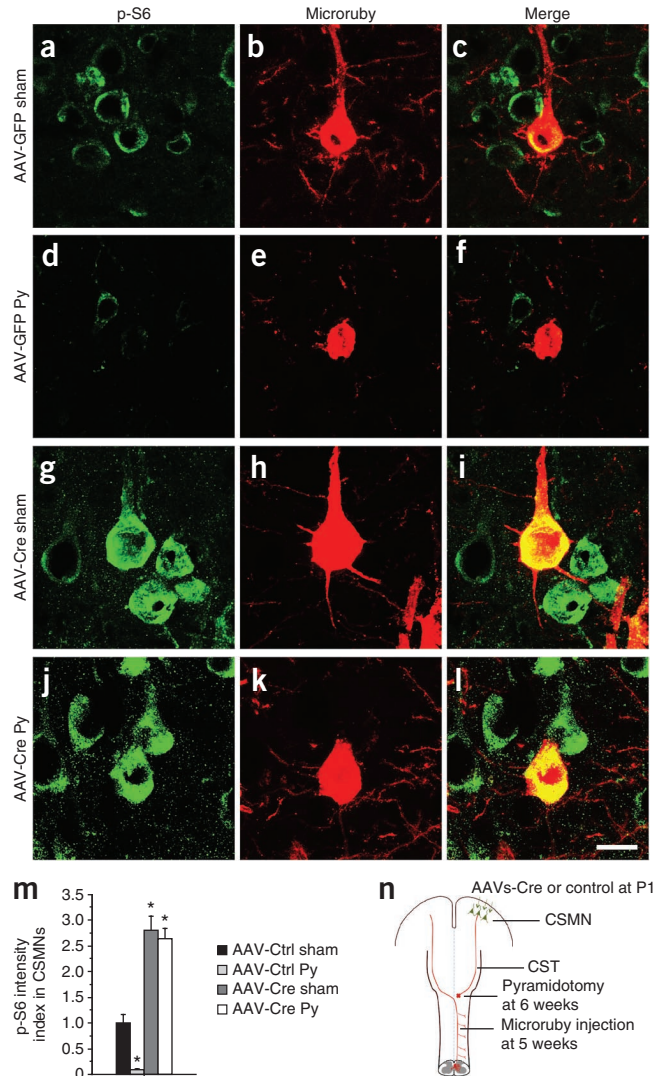
the observation that the development of CST projections is largely complete by the early postnatal stage²⁴.

We next performed pyramidotomy in adult *Pten*^{loxP/loxP} mice, which were injected neonatally with AAV-Cre or AAV-GFP. Compared with the limited sprouting in controls (**Fig. 3**), *Pten* deletion elicited extensive trans-midline sprouting of adult CST axons from the intact side into the denervated side (**Fig. 3m–r**). Thus, *Pten* deletion was sufficient for maintaining the high mTOR activity that is characteristic of young neurons in adult cortical neurons and for these neurons to launch a robust sprouting response after injury.

CST regeneration after T8 dorsal hemisection after neonatal *Pten* deletion

Sprouting of uninjured neurons might partially compensate for lost function, inducing severed axons to regenerate beyond the lesion site and to reconnect the axonal pathways that would be needed for functional recovery in more severe injuries. We asked whether *Pten* deletion would sustain a high level of mTOR activity in injured adult corticospinal neurons and elicit robust axon regeneration. Using immunohistochemistry, we found that axotomy diminished p-S6 levels in adult corticospinal neurons identified by retrograde labeling (**Fig. 2d–f,m**). Stepwise downregulation of mTOR activity, by age-dependent decline (**Fig. 1h,i**) and then an injury-triggered reduction (**Fig. 2a–f,m**), resulted in lesioned adult corticospinal neurons exhibiting low p-S6 signal, suggesting that mTOR activity was greatly reduced. Notably, AAV-Cre-mediated *Pten* deletion not only increased basal p-S6 levels (**Fig. 2g–i,m**) but also efficiently attenuated the injury-induced loss of mTOR activity in corticospinal neurons (**Fig. 2j–m**).

Having established an experimental procedure for maintaining a relatively high level of mTOR activity in adult corticospinal neurons even after injury, we set out to determine whether *Pten* deletion would enable regenerative growth of adult CST axons in two different spinal cord injury procedures (**Supplementary Fig. 4**): a dorsal hemisection, which transects all traced CST axons but spares the ventral spinal cord^{25–28}, and a complete crush model that transects all passing axons and leaves no bridge of uninjured tissue^{29,30}.



Dorsal hemisection injuries were created at T8 (**Supplementary Fig. 4**) and the CST from one hemisphere was traced 6 weeks post-injury by injecting BDA into the right sensorimotor cortex, allowing the mice to survive for another 2 weeks. Transverse sections 5 mm caudal to the lesion sites were examined. The presence of any labeled axons in the dorsal main tract and the dorsolateral tract caudal to the injury was taken as evidence of incomplete lesions and these mice were excluded from further analysis.

In nine control mice, not a single CST axon was seen extending directly through the lesion site (**Fig. 4a,b**). In two of these control mice, we found a few axons extending to the distal spinal cord via the ventral column, consistent with previous observations²⁸. Instead, characteristic dieback of CST axons from the injury site was observed (**Fig. 4a,b** and **Supplementary Fig. 5**) and individual axons had numerous retraction bulbs (**Supplementary Fig. 5**). In contrast, when PTEN was deleted, the main CST bundle extended to the very edge of the lesion margin (**Fig. 4c,d** and **Supplementary Fig. 5**) and few retraction bulbs were associated with the labeled CST axons 8 weeks after injury (**Supplementary Fig. 5**). This phenotype could be a result of either a lack of axon dieback of *Pten*-deleted neurons or resumed axon regrowth after the initial injury-induced retraction. To distinguish between these, we examined CST axons at 10 d

post-injury. Apparent dieback and large numbers of retraction bulbs were observed at this early time point in both control and *Pten*-deleted axons (**Supplementary Fig. 6**). Thus, instead of affecting the acute post-injury axonal degeneration, *Pten* deletion likely reversed the normal abortive regenerative attempts typical for injured adult CNS axons³¹ and enhanced their regrowth.

More notably, substantial numbers of labeled axons regenerated past the lesion site in all 11 *Pten*-deleted mice (**Fig. 4e–g**). Examination of the entire collection of serial sections from these mice (**Supplementary Fig. 7**) revealed two distinct routes by which labeled CST axons reached the caudal spinal cord: either directly growing through the lesion or circumventing the injury site via the spared ventral white matter (**Fig. 4e**). We estimated that approximately two-thirds of labeled axons seen in the distal spinal cord grew through the lesion site and the rest projected along the ventral white matter. Notably, CST axons that regenerated past the lesion were not restricted to one side of the distal spinal cord and instead projected bilaterally (**Supplementary Fig. 7**). This is important because normal CST projections are largely unilateral. The presence of substantial numbers of CST axons on the side contralateral to the main tract is strong evidence of regenerative growth and cannot be accounted for by spared axons.

We obtained similar results in an independent set of experiments in which the lesions were performed in a double-blind manner by an independent surgeon (**Supplementary Fig. 8**) who has previously carried out extensive analyses of possible CST regeneration in *Nogo* knockout mice³². In these experiments with control and *Pten*-deleted mice, the genotypes (AAV-Cre versus control) could be predicted by a blinded observer with great accuracy (~95%) on the basis of BDA labeling (regenerator versus nonregenerator), further supporting the highly robust effect of *Pten* deletion. Thus, the effect of *Pten* deletion was consistent and robust enough to overcome the inter-investigator surgical variability typical for experimental spinal cord injury models.

Notably, the majority of *Pten*-deleted regenerating axons projecting into the lesion site were associated with glial fibrillary acidic protein (GFAP)-positive tissue matrix (**Fig. 4c,d** and **Supplementary Fig. 9**). These GFAP-positive matrices often appeared in the superficial and medial locations of the spinal cord, which would be highly unlikely, if not impossible, to be spared in a dorsal hemisection. GFAP-positive bridges were rarely seen at a shorter time frame after injury (for example, **Supplementary Figs. 6, 10** and **11**), suggesting that these matrixes develop over time following dorsal hemisection, possibly as a consequence of an interaction between GFAP-negative cells and GFAP-positive cells at the injury site³³. However, the identity of these GFAP-positive cells or matrixes remains unknown.

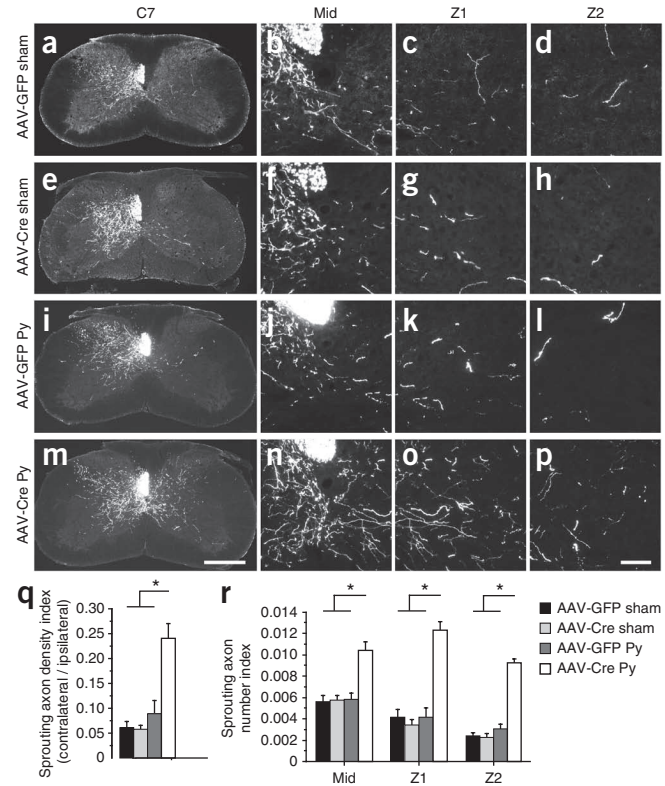


Figure 3 *Pten* deletion promotes CST sprouting in adult mice with unilateral pyramidotomy. (a–p) Representative images of C7 spinal cord transverse sections (a,e,i,m), enlarged midline (b,f,j,n), Z1 (c,g,k,o) or Z2 (d,h,l,p) regions from sham (a–h) or injured (i–p) *Pten*^{loxP/loxP} mice injected with either AAV-GFP (a–d,i–l) or AAV-Cre (e–h,m–p). AAVs were injected into the right sensorimotor cortex of P1 *Pten*^{loxP/loxP} mice, which then received a left pyramidotomy or sham lesion at 2 months. BDA was injected into the right sensorimotor cortex at 2 weeks post-injury and the mice were terminated 2 weeks later. (q) Quantification of sprouting axon density index (contralateral/ipsilateral). * $P < 0.01$, ANOVA followed by Bonferroni's *post hoc* test. (r) Quantifications of crossing axons counted in different regions of spinal cord normalized against the numbers of labeled CST axons. * $P < 0.01$, ANOVA followed by Bonferroni's *post hoc* test. We used five mice in each intact group and six mice in each pyramidotomy group. Three C7 spinal cord sections per animals were quantified. Scale bars represent 500 μ m (a,e,i,m) and 50 μ m (b–d,f–h,j–l,n–p).

CST regeneration after T8 complete crush after *Pten* deletion

A complete spinal cord crush destroys all neural tissues at the injury site (**Supplementary Fig. 4**) and is considered to be an extraordinary barrier for regeneration^{29,30}. In this model, the dura mater is not damaged and the two ends of the spinal cord do not pull apart. In mice, the lesion site is filled with a connective tissue matrix^{29,30}. Initially, the matrix was largely GFAP negative, but GFAP-positive fingers extended into the connective tissue matrix at later post-injury stages (**Supplementary Fig. 10**).

At 12 weeks post-injury, no CST axons extended into or beyond the lesion site in any of the eight control mice (**Fig. 5** and **Supplementary Fig. 12**). In contrast, numerous axons extended into the lesion sites and beyond the lesion for up to 3 mm in all eight *Pten*^{loxP/loxP} mice that received AAV-Cre injections (**Fig. 5c–e** and **Supplementary Fig. 12**). Many regenerating axons followed ectopic trajectories. For example, instead of projecting in one side of the spinal cord as did normal CST axons, regenerating axons extended bilaterally, with many of them showing tortuous projection patterns (**Supplementary Fig. 12**), indicating that they were not spared axons.

These results were obtained from mice that received an AAV-Cre injection at a neonatal age and a spinal cord crush injury at 2 months of age. Does this increased CST regeneration ability persist in cortico-spinal neurons in older mice? To assess this, we performed another set of experiments in which the same T8 spinal cord crush was performed in 5-month-old *Pten*^{loxP/loxP} mice with neonatal cortical injection of AAV-Cre or AAV-GFP. We found substantial CST regeneration at 3 months post-injury in these mice (**Supplementary Fig. 13**), similar to mice injured at 2 months (**Fig. 5** and **Supplementary Fig. 12**).

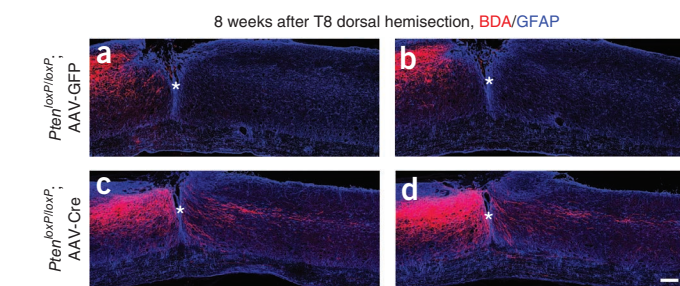


Figure 4 Increased CST regrowth in *Pten*-deleted mice after T8 dorsal hemisection. (a–d) Representative images from sagittal sections from *Pten*^{loxP/loxP} mice with right cortical injection of AAV-GFP (a,b) or AAV-Cre (c,d) at P1 and T8 dorsal hemisection at 6 weeks. BDA was injected into the right sensorimotor cortex at 6 weeks post-injury and the mice were killed 2 weeks later. The sections were stained for BDA (red) and GFAP (blue). Asterisk indicates lesion site. (e) Magnification of images in d showing two types of labeled axons growing to the distal spinal cord: growing through the lesion sites (red arrow) and sprouting through the intact ventral spinal cord (red arrowhead). Red star denotes the lesion site. (f) Quantification of the density of labeled CST axons in the spinal cord rostral to the lesion sites in two groups. * $P < 0.05$, two-way ANOVA followed by Fisher's LSD. (g) Quantification of the CST axons quantified in the spinal cord distal to the lesion sites. * $P < 0.05$, two-way ANOVA followed by Fisher's LSD. We used nine mice in the AAV-GFP group and 11 in the AAV-Cre group. We quantified four to five sections per mouse. Scale bar represents 200 μ m.

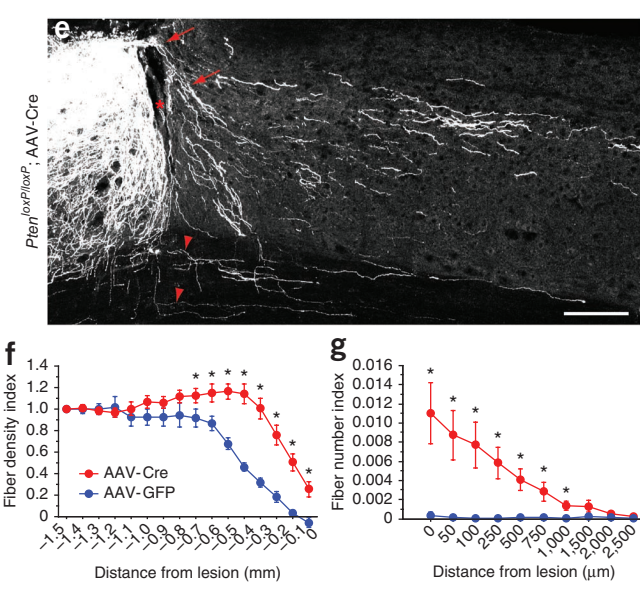


Figure 5 CST regeneration in *PTEN* deleted mice after a T8 spinal cord crush injury. (a–d) Representative images from sagittal sections showing the main dorsal CST tract (a,c) or lateral CST axons in the gray matter (b,d) in *Pten*^{loxP/loxP} mice with cortical injection of AAV-GFP (a,b) or AAV-Cre (c,d) at P1 and T8 crush injury at 6 weeks. BDA was injected into the sensorimotor cortex at 10 weeks after injury and the mice were killed 2 weeks later. The sections were stained for BDA (red) and GFAP (blue). In contrast with control mice, in which no labeled axons could be seen in or beyond the lesion site, numerous axons grew through the lesion site and were detected in the distal spinal cord (up to 3 mm). Scale bar represents 200 μ m. (e) Quantification of labeled axons in the spinal cord caudal to the lesion site in both groups. * $P < 0.05$, two-way ANOVA followed by Fisher's LSD. Eight mice in each group were used. Three sections per mouse were quantified. (f,g) Immunofluorescent images showing sections from the matrix of the lesion sites of crushed *Pten*^{loxP/loxP} mice injected with either AAV-GFP (f) or AAV-Cre (g) detected with TSA-Cy3 (for BDA) and antibody to GFAP. Scale bar represents 20 μ m. Asterisk indicates lesion site in a–d, f and g.

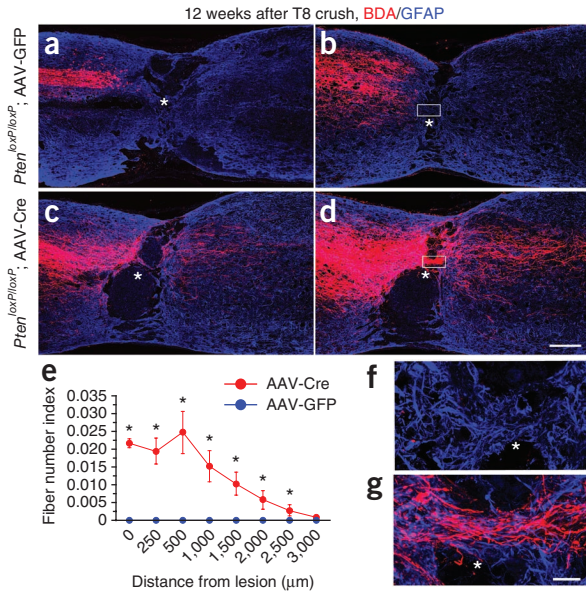
Postneonatal *Pten* deletion induces CST regeneration

Although we found no significant changes of CST numbers and projections in the spinal cord in *Pten*^{loxP/loxP} mice with neonatal AAV-Cre cortical injections (Supplementary Fig. 3), it is still possible that the upregulation of mTOR activity associated with PTEN deletion at this early stage could block developmental events that turn off axon regeneration. To assess this, we first optimized a stereotaxic injection method to introduce AAVs to the sensorimotor cortex of mice at the age of 4 weeks. AAV-Cre injections resulted in efficient Cre-dependent PLAP expression in reporter mice (Fig. 6). We estimated that AAV-Cre injection at 4 weeks, in comparison with neonatal AAV-Cre injection (Supplementary Fig. 2), resulted in Cre-dependent PLAP expression in about 25% as much cortical area, probably as a result of less efficient diffusion of injected viral particles in the more mature cortex.

We then followed introduction of AAVs into the sensorimotor cortex of *Pten*^{loxP/loxP} mice at 4 weeks with a T8 complete spinal cord crush injury at 8 weeks and analyzed CST regeneration 3 months post-injury. We still found substantial CST regeneration in the spinal cord caudal to the lesion sites (Fig. 6c–e). Thus, *Pten* deletion at both neonatal and young adult stages promoted robust CST axon regeneration past a complete spinal cord crush lesion.

Regenerating CST axons re-form synaptic structures

We next investigated whether regenerating CST axons from *Pten*-deleted corticospinal neurons are able to form synapses. For this, we analyzed the samples taken from the gray matter of the spinal



cord caudal to the lesion site in *Pten*^{loxP/loxP} mice with neonatal AAV-Cre injection and T8 crush injury at 2 months. We assessed whether BDA-labeled regenerating CST axons expressed vGlut1, a presynaptic marker for excitatory synapses^{34–36}. Some BDA-labeled bouton-like structures had vGlut1-positive patches at the tip of BDA-labeled CST collaterals (Fig. 7) and along the axonal length (Fig. 7f–h), suggesting the accumulation of the molecular machinery characteristic of a presynaptic terminal. We quantified these BDA- and vGlut1-stained bouton-like structures in similar spinal cord locations in wild-type intact mice and *Pten*-deleted mice with crush injury. The incidence of vGlut1-positive patches in regenerating CST axons was approximately two-thirds of that of CST axons in uninjured mice (Fig. 7i).

We further assessed whether BDA-labeled regenerated axons form synapses at the ultrastructural level. Sections from the spinal cords from *Pten*-deleted mice with crush injuries and BDA injections were stained for BDA and processed for electron microscopy analysis (Fig. 7j–l). We found many structures with characteristics of synapses on the basis of the presence of a contact zone with presynaptic vesicles (partially obscured by the reaction products in the labeled terminal) and a post-synaptic density (PSD; Fig. 7j,k). These results indicate that regenerating CST axons from *Pten*-deleted corticospinal neurons appear to possess the ability to reform synapses in caudal segments. Whether these synapses are functional and the identities of the neurons contacted by the regenerated axons remain unknown.

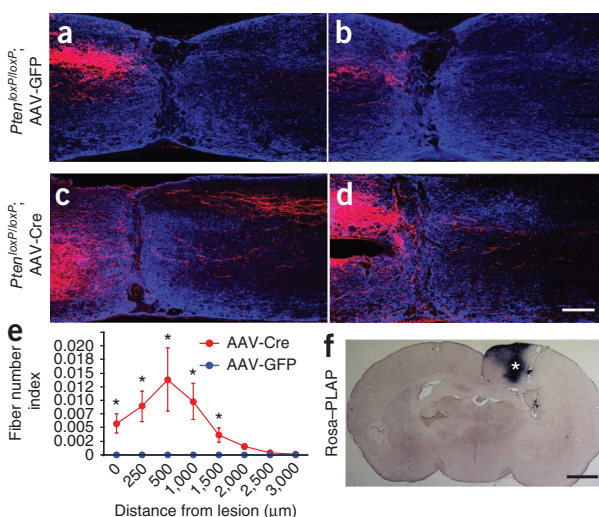
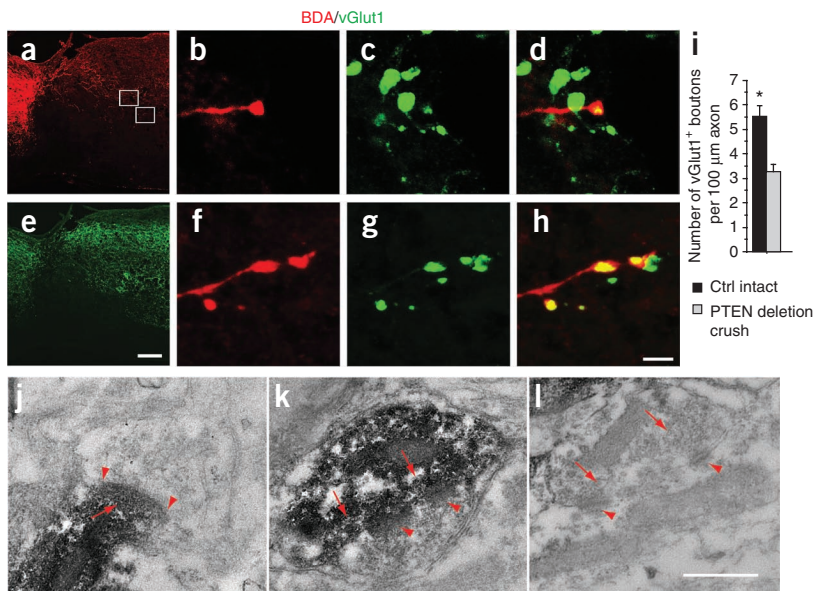


Figure 6 CST regeneration in *Pten*^{loxP/loxP} mice with AAV injection at 4 weeks and T8 spinal cord crush injury at 8 weeks. (a–d) Representative images from sagittal sections showing the main dorsal CST tract (a,c) or lateral CST axons in the gray matter (b,d) in *Pten*^{loxP/loxP} mice with cortical injection of AAV-GFP (a,b) or AAV-Cre (c,d) at 4 weeks and T8 crush injury at 8 weeks. BDA was injected into the sensorimotor cortex at 10 weeks after injury and the mice were killed 2 weeks later. The sections were stained for BDA (red) and GFAP (blue). Scale bar represents 200 μ m. (e) Quantification of labeled axons in the spinal cord caudal to the lesion site in both groups. * $P < 0.05$, two-way ANOVA followed by Fisher's LSD. Five mice in each group were used. Three sections per mouse were quantified. (f) PLAP staining of a cortical section from a reporter mouse with AAV-Cre injection at the age of 4 weeks. Asterisk indicates injection site. By examining different sections covering entire hindlimb sensorimotor cortex, we estimated that area that was PLAP positive in these mice was about 20% that of the reporter mice with neonatal AAV-Cre injection. Scale bar represents 1 mm.

Figure 7 Regenerating CST axons after *Pten* deletion form synapse-structures in spinal segments caudal to a crush injury. (a,b) Sagittal sections from *Pten*^{loxP/loxP} mice injected with AAV-Cre at P1, T8 spinal cord crush at the age of 6 weeks, BDA tracing at the age of 16 weeks and killed at the age 18 weeks were analyzed for BDA (a) and vGlut1 (b) signals. Antibody to vGlut1 labeled synaptic boutons of both CST axons and sensory axons, consistent with previous results^{34–36}. (c–h) Representative examples of BDA-labeled boutons (c,f) colocalizing with vGlut1 (d,g) and their merged images (e,h) from the gray matter of the spinal cord caudal to the crush site (squares in a). Scale bars represent 200 μ m (a,e) and 5 μ m (b–d,f–h). (i) Frequencies of vGlut1-positive boutons in BDA-labeled axons quantified mostly from the intermediate zone of the thoracic spinal cord gray matter in both intact control and *Pten*^{loxP/loxP} mice injected with AAV-Cre. Both the BDA-labeled axonal lengths and the BDA-positive, vGlut1-positive boutons from 15 sections from three mice in each group were quantified. In crushed PTEN-deletion mice, we found BDA and vGlut1 double-positive synapses approximately 60% as frequently as in intact control mice. Student's *t* test, **P* < 0.05. (j–l) Representative electron microscope images showing two synaptic structures formed by BDA-labeled axons (j,k) and a nearby unlabeled control synapse (l). In spinal neurons, the synaptic contact region often has patches of PSD, which is the case in the synapse in k. In j, the PSD is continuous between the arrows. Arrowheads indicate synaptic vesicles. Scale bar represents 1 μ m (j,k,l).



DISCUSSION

Together, our results indicate that *Pten* deletion enables injured adult corticospinal neurons to mount a robust regenerative response that, to the best of our knowledge, has not been observed previously in the mammalian spinal cord. Both compensatory sprouting of intact CST axons and regenerative growth of injured CST axons were markedly increased by *Pten* deletion, suggesting that these two forms of regrowth have similar underlying mechanisms. PTEN inactivation is known to activate different downstream pathways, such as Akt and mTOR signaling, and inhibit other signaling molecules, such as GSK-3 (refs. 21,37,38) and PIP3 (ref. 39). In cortical neurons, mTOR activity undergoes a development-dependent downregulation and axotomy further diminishes mTOR activity. *Pten* deletion in these neurons could increase mTOR activity and promote their regrowth ability. Together with our previous findings in retinal ganglion neurons¹⁸, our results indicate that mTOR activity is critical for determining the regrowth ability of CNS neurons. Because mTOR is a central regulator of cap-dependent protein translation²¹, it is likely that neuronal growth competence is dependent on the capability of new protein synthesis, which provides building blocks for axonal regrowth. Other *Pten* deletion-induced effects, such as increased axonal transport resulting from the inactivation of GSK-3, might also be involved.

Our results also indicate that regenerating CST axons from *Pten*-deleted corticospinal neurons are able to reform synapses in the spinal cord caudal to the lesion site. CST axons that regenerate after *Pten* deletion extend bilaterally, in contrast with normal CST axons that extend unilaterally; the extent to which these regenerating axons can make synaptic connections with their original targets is unknown. In some species, such as the larval lamprey⁴⁰ and goldfish⁴¹, axons that regenerate past a spinal cord lesion fail to reach their original targets but make synapses that allow functional recovery.

Notably, despite robust regenerative growth of CST axons rostral to a spinal cord injury in *Pten*-deleted mice, many robustly growing axons failed to penetrate into the GFAP-negative area at the lesion site. This suggests that the lesion site, and particularly the GFAP-negative area,

remains a formidable barrier to regenerating axons from PTEN-deleted corticospinal neurons. Thus, a combination of PTEN deletion and other strategies, such as neutralizing extracellular inhibitors at the lesion site^{42,43} and bridging the lesion site with permissive grafts^{44,45}, may further promote maximal axon regeneration after spinal cord injury.

Taken together, our results indicate that immature neurons with high regenerative ability^{46,47} have a high level of mTOR activity. mTOR activity undergoes a development-dependent downregulation in many types of CNS neurons and corticospinal neurons, suggesting that lack of mTOR activation is a general neuron-intrinsic mechanism underlying the diminished regenerative ability in the adult CNS. Together with optic nerve regeneration observed after PTEN deletion¹⁸, our results strongly support the idea that reactivation of the mTOR pathway allows adult neurons to regain some of the growth capacities characteristic of young neurons. This ‘rejuvenation’ strategy may be widely applicable for promoting successful regeneration following many types of injuries or traumas in the adult CNS.

METHODS

Methods and any associated references are available in the online version of the paper at <http://www.nature.com/natureneuroscience/>.

Note: Supplementary information is available on the Nature Neuroscience website.

ACKNOWLEDGMENTS

We thank F. Wang for providing Rosa-stop-PLAP mice and M. Greenberg, M. Tessier-Lavigne and C. Woolf for reading the manuscript. This work was supported by grants from Wings for Life (K.L. and Z.H.), the Dr. Miriam and Sheldon G. Adelson Medical Research Foundation (Z.H.), the Craig H. Neilsen Foundation (Y.L. and K.K.P.), the National Institute of Neurological Disorders and Stroke (Z.H., B.Z. and O.S.), the International Spinal Research Trust (Z.H.) and a private contribution to the Reeve-Irvine Research Center (O.S.). R.W. is the recipient of a predoctoral fellowship from the National Institute of Neurological Disorders and Stroke.

AUTHOR CONTRIBUTIONS

K.L., Y.L., J.K.L., R.S., R.W., I.S.-K., A.T., K.K.P., D.J., B.C., B.X., L.C. and O.S. performed the experiments and analyzed the data. K.L., J.K.L., O.S., B.Z. and Z.H. drafted and edited the manuscript.

COMPETING FINANCIAL INTERESTS

The authors declare competing financial interests: details accompany the full-text HTML version of the paper at www.nature.com/natureneuroscience/.

Published online at <http://www.nature.com/natureneuroscience/>.

Reprints and permissions information is available online at <http://www.nature.com/reprintsandpermissions/>.

1. Raineteau, O. & Schwab, M.E. Plasticity of motor systems after incomplete spinal cord injury. *Nat. Rev. Neurosci.* **2**, 263–273 (2001).
2. Blesch, A. & Tuszyński, M.H. Spinal cord injury: plasticity, regeneration and the challenge of translational drug development. *Trends Neurosci.* **32**, 41–47 (2009).
3. Zheng, B., Lee, J.K. & Xie, F. Genetic mouse models for studying inhibitors of spinal axon regeneration. *Trends Neurosci.* **29**, 640–646 (2006).
4. Deumens, R., Koopmans, G.C. & Joosten, E.A. Regeneration of descending axon tracts after spinal cord injury. *Prog. Neurobiol.* **77**, 57–89 (2005).
5. Thallmair, M., Metz, G.A., ZGraggen, W.J., Raineteau, O., Kartje, G.L. & Schwab, M.E. Neurite growth inhibitors restrict plasticity and functional recovery following corticospinal tract lesions. *Nat. Neurosci.* **1**, 124–131 (1998).
6. Cafferty, W.B. & Strittmatter, S.M. The Nogo-Nogo receptor pathway limits a spectrum of adult CNS axonal growth. *J. Neurosci.* **26**, 12242–12250 (2006).
7. Case, L.C. & Tessier-Lavigne, M. Regeneration of the adult central nervous system. *Curr. Biol.* **15**, R749–R753 (2005).
8. Schnell, L. & Schwab, M.E. Axonal regeneration in the rat spinal cord produced by an antibody against myelin-associated neurite growth inhibitors. *Nature* **343**, 269–272 (1990).
9. Savio, T. & Schwab, M.E. Lesioned corticospinal tract axons regenerate in myelin-free rat spinal cord. *Proc. Natl. Acad. Sci. USA* **87**, 4130–4133 (1990).
10. García-Alías, G., Barkhuyzen, S., Buckle, M. & Fawcett, J.W. Chondroitinase ABC treatment opens a window of opportunity for task-specific rehabilitation. *Nat. Neurosci.* **12**, 1145–1151 (2009).
11. Leaver, S.G. *et al.* AAV-mediated expression of CNTF promotes long-term survival and regeneration of adult rat retinal ganglion cells. *Gene Ther.* **13**, 1328–1341 (2006).
12. Schnell, L., Schneider, R., Kolbeck, R., Barde, Y.A. & Schwab, M.E. Neurotrophin-3 enhances sprouting of corticospinal tract during development and after adult spinal cord lesion. *Nature* **367**, 170–173 (1994).
13. Hieber, G.W., Khodarahmi, K., McGraw, J., Steeves, J.D. & Tetzlaff, W. Brain-derived neurotrophic factor applied to the motor cortex promotes sprouting of corticospinal fibers, but not regeneration into a peripheral nerve transplant. *J. Neurosci. Res.* **69**, 160–168 (2002).
14. Hollis, E.R. II, Lu, P., Blesch, A. & Tuszyński, M.H. IGF-I gene delivery promotes corticospinal neuronal survival, but not regeneration, after adult CNS injury. *Exp. Neurol.* **215**, 53–59 (2009).
15. David, S. & Aguayo, A.J. Axonal elongation into peripheral nervous system “bridges” after central nervous system injury in adult rats. *Science* **214**, 931–933 (1981).
16. Richardson, P.M., Issa, V.M. & Aguayo, A.J. Regeneration of long spinal axons in the rat. *J. Neurocytol.* **13**, 165–182 (1984).
17. Bregman, B.S., Kunkel-Bagden, E., McAtee, M. & O'Neill, A. Extension of the critical period for developmental plasticity of the corticospinal pathway. *J. Comp. Neurol.* **282**, 355–370 (1989).
18. Park, K.K. *et al.* Promoting axon regeneration in the adult CNS by modulation of the PTEN/mTOR pathway. *Science* **322**, 963–966 (2008).
19. Bareyre, F.M. *et al.* The injured spinal cord spontaneously forms a new intraspinal circuit in adult rats. *Nat. Neurosci.* **7**, 269–277 (2004).
20. Weidner, N., Ner, A., Salimi, N. & Tuszyński, M.H. Spontaneous corticospinal axonal plasticity and functional recovery after adult central nervous system injury. *Proc. Natl. Acad. Sci. USA* **98**, 3513–3518 (2001).
21. Ma, X.M. & Blenis, J. Molecular mechanisms of mTOR-mediated translational control. *Nat. Rev. Mol. Cell Biol.* **10**, 307–318 (2009).
22. Groszer, M. *et al.* Negative regulation of neural stem/progenitor cell proliferation by the Pten tumor suppressor gene *in vivo*. *Science* **294**, 2186–2189 (2001).
23. Hasegawa, H. & Wang, F. Visualizing mechanosensory endings of TrkB-expressing neurons in HS3ST2-hPLAP mice. *J. Comp. Neurol.* **511**, 543–556 (2008).
24. Bareyre, F.M., Kerschensteiner, M., Misgeld, T. & Sanes, J.R. Transgenic labeling of the corticospinal tract for monitoring axonal responses to spinal cord injury. *Nat. Med.* **11**, 1355–1360 (2005).
25. Simonen, M. *et al.* Systemic deletion of the myelin-associated outgrowth inhibitor Nogo-A improves regenerative and plastic responses after spinal cord injury. *Neuron* **38**, 201–211 (2003).
26. Kim, J.E., Li, S., GrandPre, T., Qiu, D. & Strittmatter, S.M. Axon regeneration in young adult mice lacking Nogo-A/B. *Neuron* **38**, 187–199 (2003).
27. Zheng, B. *et al.* Lack of enhanced spinal regeneration in Nogo-deficient mice. *Neuron* **38**, 213–224 (2003).
28. Steward, O. *et al.* Regenerative growth of corticospinal tract axons via the ventral column after spinal cord injury in mice. *J. Neurosci.* **28**, 6836–6847 (2008).
29. Fujiki, M., Zhang, Z., Guth, L. & Steward, O. Genetic influences on cellular reactions to spinal cord injury: activation of macrophages/microglia and astrocytes is delayed in mice carrying a mutation (*WldS*) that causes delayed Wallerian degeneration. *J. Comp. Neurol.* **371**, 469–484 (1996).
30. Inman, D.M. & Steward, O. Ascending sensory, but not other long-tract axons, regenerate into the connective tissue matrix that forms at the site of a spinal cord injury in mice. *J. Comp. Neurol.* **462**, 431–449 (2003).
31. Tom, V.J., Steinmetz, M.P., Miller, J.H., Doller, C.M. & Silver, J. Studies on the development and behavior of the dystrophic growth cone, the hallmark of regeneration failure, in an *in vitro* model of the glial scar and after spinal cord injury. *J. Neurosci.* **24**, 6531–6539 (2004).
32. Lee, J.K. *et al.* Reassessment of corticospinal tract regeneration in Nogo-deficient mice. *J. Neurosci.* **29**, 8649–8654 (2009).
33. Bundesen, L.Q., Scheel, T.A., Bregman, B.S. & Kromer, L.F. Ephrin-B2 and EphB2 regulation of astrocyte-meningeal fibroblast interactions in response to spinal cord lesions in adult rats. *J. Neurosci.* **23**, 7789–7800 (2003).
34. Maier, I.C. *et al.* Constraint-induced movement therapy in the adult rat after unilateral corticospinal tract injury. *J. Neurosci.* **28**, 9386–9403 (2008).
35. Varoqui, H., Schäfer, M.K., Zhu, H., Weihe, E. & Erickson, J.D. Identification of the differentiation-associated Na⁺/Pi transporter as a novel vesicular glutamate transporter expressed in a distinct set of glutamatergic synapses. *J. Neurosci.* **22**, 142–155 (2002).
36. Persson, S. *et al.* Distribution of vesicular glutamate transporters 1 and 2 in the rat spinal cord, with a note on the spinocervical tract. *J. Comp. Neurol.* **497**, 683–701 (2006).
37. Zhou, F.Q., Zhou, J., Dedhar, S., Wu, Y.H. & Snider, W.D. NGF-induced axon growth is mediated by localized inactivation of GSK-3beta and functions of the microtubule plus end binding protein APC. *Neuron* **42**, 897–912 (2004).
38. Park, K.K., Liu, K., Hu, Y., Kanter, J.L. & He, Z. PTEN/mTOR and axon regeneration. *Exp. Neurol.* **223**, 45–50 (2010).
39. Zhao, M. *et al.* Electrical signals control wound healing through phosphatidylinositol-3-OH kinase-gamma and PTEN. *Nature* **442**, 457–460 (2006).
40. Yin, H.S. & Selzer, M.E. Axonal regeneration in lamprey spinal cord. *J. Neurosci.* **3**, 1135–1144 (1983).
41. Bernstein, J.J. & Gelderd, J.B. Synaptic reorganization following regeneration of goldfish spinal cord. *Exp. Neurol.* **41**, 402–410 (1973).
42. García-Alías, G., Barkhuyzen, S., Buckle, M. & Fawcett, J.W. Chondroitinase ABC treatment opens a window of opportunity for task-specific rehabilitation. *Nat. Neurosci.* **12**, 1145–1151 (2009).
43. Houle, J.D. *et al.* Combining an autologous peripheral nervous system “bridge” and matrix modification by chondroitinase allows robust, functional regeneration beyond a hemisection lesion of the adult rat spinal cord. *J. Neurosci.* **26**, 7405–7415 (2006).
44. Alto, L.T. *et al.* Chemotropic guidance facilitates axonal regeneration and synapse formation after spinal cord injury. *Nat. Neurosci.* **12**, 1106–1113 (2009).
45. Pearse, D.D. *et al.* cAMP and Schwann cells promote axonal growth and functional recovery after spinal cord injury. *Nat. Med.* **10**, 610–616 (2004).
46. Kennard, M.A. age and other factors in motor recovery from precentral lesions in monkeys. *Am. J. Physiol.* **115**, 138–146 (1936).
47. Berger, W. Characteristics of locomotor control in children with cerebral palsy. *Neurosci. Biobehav. Rev.* **22**, 579–582 (1998).

ONLINE METHODS

Mice and surgeries. All experimental procedures were performed in compliance with animal protocols approved by the Institutional Animal Care and Use Committee at Children's Hospital, Boston. AAV preparation was described previously¹⁸.

For AAV injection, neonatal *Pten*^{loxP/loxP} mice were cryoanesthetized and injected with 2 μ l of either AAV-Cre or AAV-GFP into the right sensorimotor cortex using a nanoliter injector attached to a fine glass pipette. Mice were then placed on a warming pad and returned to their mothers after regaining normal color and activity. For 4-week-old mice, a total of 1.5 μ l of AAV-Cre or AAV-GFP was injected into the hind limb sensorimotor cortex at three sites (coordinates from bregma in mm: anterior-posterior/medial-lateral/dorsal-ventral, 0.0/1.5/0.5, -0.5/1.5/0.5, -1.0/1.5/0.5). The mice were placed on a warming blanket held at 37 °C until fully awake and received a spinal cord lesion 4 weeks later.

For pyramidotomy, mice were anesthetized with ketamine/xylazine. The procedure is similar to that described previously^{19,20}. Briefly, an incision was made at the left side of the trachea. Blunt dissection was performed to expose the skull base and a craniotomy in the occipital bone allowed for access to the medullary pyramids. The left or right pyramid was cut with a fine scalpel medially up to the basilar artery. The wound was closed in layers with 6.0 sutures. The mice were placed on soft bedding on a warming blanket held at 37 °C until fully awake. We traced the intact CST 2 weeks later with BDA.

The procedure for T8 dorsal hemisection was similar to that described previously^{24–28}. Briefly, a midline incision was made over the thoracic vertebrae. A T8 laminectomy was performed. To produce a dorsal hemisection injury, we first cut the dorsal spinal cord with a pair of microscissors to the depth of 0.8 mm and then drew a fine microknife bilaterally across the dorsal aspect of the spinal cord. The muscle layers were sutured and the skin was secured with wound clips. The mice were placed on soft bedding on a warming blanket held at 37 °C until fully awake. Urine was expressed by manual abdominal pressure twice daily until mice regained reflex bladder function. We injected BDA into the sensorimotor cortex to trace the CST 6 weeks post-injury.

The procedure of T8 spinal cord crush is similar to what was described previously^{29,30} with modifications. Briefly, a midline incision was made over the thoracic vertebrae. A T8 laminectomy was performed. The exposed cord was crushed for 2 s with modified no. 5 jeweler's forceps, keeping the dura intact. The muscle layers were sutured and the skin was secured with wound clips. The mice were placed on soft bedding on a warming blanket held at 37 °C until fully awake. Urine was expressed by manual abdominal pressure twice daily for the entire duration of the experiment. At 10 weeks post-injury, the CST was traced with BDA.

BDA tracing. To label CST axons by anterograde tracing, we injected a total of 1.6 μ l of BDA (10%, Invitrogen) into sensorimotor cortex at four sites (anterior-posterior coordinates from bregma in mm: 1.0/1.5, 0.5/1.5, -0.5/1.5, -1.0/1.5, all at a depth of 0.5 mm into cortex). Mice were kept for an additional 2 weeks before being killed.

Microruby retrograde labeling. Labeling was carried out as described previously with modifications^{48,49}. Briefly, a C3 laminectomy was performed and 1 μ l of Microruby tracer (3,000 molecular weight, 5%, Invitrogen) was injected into the dorsal CST at the C3 spinal cord in 10 min. The pyramidotomy or sham surgery was performed 1 week later. The intensities of p-S6 signals in microruby-labeled corticospinal neurons were measured 1 week later using the Analyze Particle Tool in ImageJ (US National Institutes of Health).

Preparation for histology and immunohistochemistry. Mice were given a lethal dose of anesthesia and transcardially perfused with 4% paraformaldehyde. Brains and spinal cords were isolated and post-fixed in the same fixative overnight at 4 °C. Tissues were cryoprotected via increasing concentrations of sucrose. After embedding into OCT compound, the samples were snap frozen in dry ice. Serial sections (25 μ m) were collected and stored at -20 °C until processed. Coronal sections of the sensorimotor cortex were cut for either p-S6 or PLAP staining. Coronal sections of the lower medulla were cut for counting BDA-labeled CST fibers. Transverse sections of intact spinal cords at identified levels (C4, C7 and T8) were collected to examine the projection pattern of CST axons. For mice with pyramidotomy, lesion sites at the medulla were carefully examined. Transverse sections of the cervical spinal cord were stained with antibody to PKC γ (Santa Cruz Biotechnology, sc-211, 1:100) to further examine the completeness of the

lesion (data not shown). Mice with incomplete lesion were excluded from the study. For assessing the extent of CST sprouting, serial sections of C7 spinal cords were cut in the transverse plane. For mice with T8 lesion, serial sections of the spinal cord region containing the lesion site were cut in the sagittal plane. Transverse sections of the caudal cord (5 mm and 3 mm to the lesion, respectively) were taken to exclude incomplete lesions.

Immunofluorescence staining of the spinal cord, cortex and medulla. Immunostaining was performed following standard protocols. All antibodies were diluted in a solution consisting of 10% normal goat serum (NGS) and 1% Triton X-100 in phosphate-buffered saline (PBS). We used rabbit antibodies to p-S6 (Ser235/236) (1:200, Cell Signaling Technology) and rabbit antibodies to GFAP (1:1,000, DAKO). Sections were incubated with primary antibodies overnight at 4 °C and washed three times for 10 min with PBS. Secondary antibodies (Alexa 488-conjugated goat antibody to rabbit) were then applied and incubated for 1 h at 20–25 °C. To detect BDA-labeled fibers, BDA staining was performed by incubating the sections in PBS containing streptavidin-horseradish peroxidase. The remaining staining procedure was performed according to the protocol provided by TSA Cyanine 3 system (Perkin Elmer).

Preparation for electron microscopy. Two mice with T8 crush injuries received unilateral injections of BDA into the sensorimotor cortex at 10 weeks post-injury and were perfused with 4% paraformaldehyde 2 weeks later. An approximately 8-mm segment of the spinal cord containing the lesion site was sectioned in the sagittal plane on a vibratome at 50 μ m. Sections were incubated for 1 h with avidin and biotinylated horseradish peroxidase (Vectastain ABC kit, Vector Laboratories), washed in PBS and then reacted with DAB in 50 mM Tris buffer, pH 7.6, 0.024% hydrogen peroxide and 0.5% nickel chloride. The sections were examined under a light microscope while still wet. Serial sections with BDA-labeled axons caudal to the injury were selected for electron microscopic analysis.

The selected sections were rinsed in 0.1 M cacodylate buffer and post-fixed with 1% osmium tetroxide in 0.1 M cacodylate buffer for 1 h, rinsed in double-distilled H₂O for 2 × 10 min, dehydrated in increasing serial dilutions of ethanol (70%, 85%, 95% and 100% × 2) for 10 min each, put in propylene oxide (intermediate solvent) for 2 × 10 min, and incubated in propylene oxide/Spurr's resin (1:1 mix) for 30 min and in Spurr's resin overnight. Sections were flat embedded between two sheets of Aclar film and polymerized overnight at 60 °C.

Images were taken of each section and imported into Adobe Photoshop. Tracings were made of the BDA-labeled axons present in each image. The tracings were then aligned and collapsed into a single image so as to reveal the BDA-labeled axons in the collection of sections. One section of the series was chosen for electron microscopic analysis and a collection of bouton-like swellings on the regenerated axons were identified in advance. Ultrathin 60-nm-thick sections were cut, mounted on copper grids and viewed using a JEOL 1400 electron microscope. Individual BDA-labeled boutons were then located and assessed at the electron microscopic level.

Axonal counting and quantifications. For quantifying total labeled CST axon, BDA-labeled CST fibers were counted at the level of medulla oblongata 1 mm proximal to the pyramidal decussation. Axons were counted in four rectangular areas (9,506 μ m²) per section on two adjacent sections. The number of labeled axons was calculated by multiplying by the total area.

For the groups of pyramidotomy, digital images of C7 spinal cord transverse sections were collected using a Nikon fluorescence microscope under a 4× objective. Densitometry measurement on each side of the gray matter was taken using Metamorph software, after being subthresholded to the background and normalized by area. The outcome measure of the sprouting density index was the ratio of contralateral and ipsilateral counts. At least three sections were measured for each mouse.

To quantify the number of sprouting axons, we drew a horizontal line through the central canal and across the lateral rim of the gray matter. Three vertical lines were then drawn to divide the horizontal line into three equal parts, starting from the central canal to the lateral rim. Only fibers crossing the three lines were counted in each section. The results were presented after normalization with the number of counted CST fibers at the medulla level. At least three sections were counted for each mouse.



In mice with T8 dorsal hemisection, digital images were taken at the CST end by using a confocal microscope (Zeiss, LSM510) under a 63 \times objective to quantify the number of retraction bulbs. The number of bulbs was counted in a 21,389- μm^2 square and normalized by the number of BDA labeled CST at the medulla. At least three sections with the main CST per animal were examined. The results were presented as the number of retraction bulbs per 0.1 mm 2 per labeled CST.

The density of sprouting fibers of the main CST rostral to the lesion site was analyzed quantitatively using digital images taken with a Nikon fluorescence microscope under a 4 \times objective. A series of rectangular segments 100 μm wide and high covering the dorsal-ventral aspect of the cord were superimposed onto the sagittal sections, starting from 1.5 mm rostral up to the lesion center. After subtracting the background (the most caudal part of the section), the pixel value of each segment was normalized by dividing with the first segment (1.5 mm rostral). The results were presented as a ratio at different distances (fiber density index). Every other section of the whole spinal cord was stained. We quantified 3–4 sections with main CST per mouse.

The number of fibers caudal to the lesion was analyzed with a fluorescence microscope. The number of intersections of BDA-labeled fibers with a dorsal-ventral line positioned at a defined distance caudal from the lesion center was counted under a 40 \times objective. Every other section of the whole spinal cord was stained. Fibers were counted on 3–4 sections with the main dorsal CST and 1–3 lateral sections with collaterals in the gray matter. The number of counted fibers was normalized by the number of labeled CST axons in the medulla and divided

by the number of evaluated sections. This resulted in the number of CST fibers per labeled CST axons per section at different distances (fiber number index).

For the mice with T8 crush, the number of fibers caudal to the lesion was analyzed with a fluorescence microscope. The number of intersections of BDA-labeled fibers with a dorsal-ventral line positioned at a defined distance caudal from the lesion center was counted under a 40 \times objective. Every other section of the whole spinal cord was stained. Fibers were counted on three sections with the main dorsal CST. The number of counted fibers was normalized by the number of labeled CST axons in the medulla and divided by the number of evaluated sections. This resulted in the number of CST fibers per labeled CST axon per section at different distances (fiber number index).

Statistical analysis. Two-tailed Student's *t* test was used for the single comparison between two groups. The rest of the data were analyzed using one-way or two-way ANOVA depending on the appropriate design. *Post hoc* comparisons were carried out only when a main effect showed statistical significance. *P* values of multiple comparisons were adjusted using Bonferroni's correction. All analyses were conducted through StatView.

48. Courtine, G. *et al.* Recovery of supraspinal control of stepping via indirect propriospinal relay connections after spinal cord injury. *Nat. Med.* **14**, 69–74 (2008).
49. Arlotta, P. *et al.* Neuronal subtype-specific genes that control corticospinal motor neuron development *in vivo*. *Neuron* **45**, 207–221 (2005).